

5,10,15,20-Tetrakis (pentafluorophenyl) Porphinatoiron (III) Chloride의 분자구조 및 그 유도체들의 F-19 NMR 구조연구

宋柄虎* · 朴光用[†] · 俞炳洙[‡]

*선문대학교 화학과 [†]중앙대학교 화공과

[‡]원광대학교 화학과

(1997. 7. 5 접수)

Molecular Structure of 5,10,15,20-Tetrakis (pentafluorophenyl) Porphinatoiron (III) Chloride and F-19 NMR Investigation of Its Derivatives

Byungho Song*, Kwangyong Park[†], and Byungsoo Yu[‡]

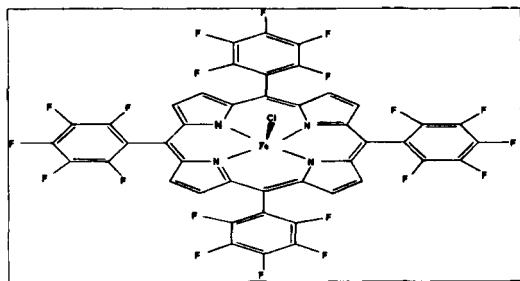
*Department of Chemistry Sun Moon University Asan City, Chung Nam

[†]Department of Chemical Engineering, JoongAng University, Seoul

[‡]Department of Chemistry, WonKwang University, Iksan, Chnubuk

(Received July 5, 1997)

Multiple halogenation of the tetraarylporphyrins serves to make the ring system relatively electron deficient. The iron and manganese complexes of these electron-deficient porphyrin provide efficient and robust oxidative catalysts for functionalization of unreactive hydrocarbons.¹ Surprisingly, the phenyl-fluorinated porphyrins also stabilize high-valent metal ions such as the iron (V) state.²



In order to compensate for the diminished electron density supplied by the porphyrin ring, the metal ion assumes a relatively higher affinity for axial ligand binding. This is reflected, for example, in the coordination of weak anionic ligands to the iron(II) form of the title compound.³ A logical question can be raised as to the effect of these elec-

tronic properties on metal-ligand atom bond distances. One might anticipate relatively shortened axial ligand-metal bond distances, and elongated pyrrole nitrogen-metal distances for the electron-deficient metalloporphyrin complexes.

The NMR spectra of paramagnetic iron porphyrin species are particularly high in information content, and such spectra may be utilized for electronic and molecular structural analysis. Solution structural identification is especially important with regard to the observation of axial ligand signals. Proton and deuterium resonance values with considerations of linewidths provide a diagnostic means for identification of iron porphyrin oxidation, spin and ligation states.⁴⁻⁶ Well-resolved carbon-13 NMR spectra of the paramagnetic iron porphyrins are also utilized for structural assignments and detailed isotropic-shift analysis.^{5,7}

The proton and deuterium NMR chemical shift value for the pyrrole resonance of paramagnetic metallo-tetraarylporphyrins has proven to be of considerable utility in definition of the electronic structures. However, phenyl proton NMR resonances of the iron tetraarylporphyrins provide less informa-

tion for elucidation of the iron porphyrin chemistry due to the relatively small dispersion of signals. Improved dispersion of fluorine-19 signals in phenyl-fluorinated iron porphyrin complexes is demonstrated in this report for various spin and oxidation states of iron tetrakis (pentafluorophenyl) porphyrin complexes. The iron tetrakis (pentafluorophenyl) porphyrin has unique properties in that the electron-deficient porphyrin induces a high affinity for axial ligands, efficiently stabilizes high-valent iron porphyrin complexes,⁸ and also serves as an efficient catalyst for oxidation of hydrocarbons.⁹⁻¹¹ Empirical and theoretical correlation of F-19 NMR chemical shifts and iron porphyrin electronic structures will facilitate the continuing utilization of electron-deficient fluorinated iron porphyrin compounds.

EXPERIMENTAL

Materials

Chlorinated solvents were purified by previously reported methods.¹² Toluene and dimethylsulfoxide (DMSO) were purchased as distilled-in-glass solvents and further purified by modifications of published methods.¹³ Solvents were degassed after or during purification either by purging with nitrogen or by the freeze-pump-thaw method. Deuterated solvents (toluene- d_8 , DMSO- d_6 , CD_2Cl_2) were purchased from Aldrich, and deoxygenated by the freeze-pump-thaw method. Solvents were stored in the argon atmosphere of a dry box.

Methyl-, ethyl- and propylmagnesium bromide and butyl- and phenyllithium were purchased from Aldrich Co. as tetrahydrofuran (THF) or diethyl ether solutions and used without purification. Solid tetrabutylammonium fluoride, $(Bu_4N)F \cdot 3H_2O$, and tetrabutylammonium hydroxide, $(Bu_4N)OH$, as a 1.0 M solution in methanol were purchased from Aldrich.

Iron porphyrin synthesis

Tetrakis(pentafluorophenyl) porphyrin, $(F_{20}-TPPH_2)$, and chloroiron(III) tetrakis (pentafluorophenyl) porphyrin, $(F_{20}-TPP)Fe(III)Cl$, were purchased from Aldrich. Alkyl- and aryliron(III) por-

phyrins were prepared by stoichiometric addition of alkylolithium, aryllithium or alkylmagnesium bromide to the toluene solutions of the chloroiron(III) porphyrin complexes.¹⁴ Hydroxoiron(III) tetrakis (pentafluorophenyl) porphyrin complex, $(F_{20}-TPP)Fe(III)OH$, was generated from $(F_{20}-TPP)Fe(II)$ in toluene solution. Addition of O_2 to $(F_{20}-TPP)Fe(II)$ initially produces hydroxoiron(III) porphyrin, $(F_{20}-TPP)Fe(III)OH$, and these compounds slowly converts to the dinuclear μ -oxoiron(III) porphyrin in 72 hours in toluene solution. The μ -oxoiron(III) porphyrin precipitated from toluene solution due to the low solubility in this solvent. Precipitated solid product was separated by filtration through a medium glass frit. Re-dissolution of the solid product in CD_2Cl_2 and examination by proton NMR spectroscopy revealed the 14.0 ppm pyrrole proton signal characteristic of $(F_{20}-TPP)Fe(III)-O-Fe(III)(F_{20}-TPP)$.¹⁵ Fluoro- and hydroxoiron(II) porphyrin anionic complexes were prepared by addition of the respective tetrabutylammonium salt to the square-planar iron(II) porphyrin.^{16,17} Crystalline iron(II) tetrakis(pentafluorophenyl) porphyrins, $(F_{20}-TPP)Fe(II)$ and $(F_{20}-TPP)Fe(II)(THF)_2$, were prepared in the dry box by mercury-activated zinc powder reduction of the chloroiron(III) complex in toluene and tetrahydrofuran solutions, respectively.¹⁸ Iron (II) tetrakis(pentafluorophenyl) porphyrins bis-coordinated by CN and piperidine and mono-ligated by Cl, CH_3CO_2 and 2-methylimidazole were prepared by addition of excess NaCN and piperidine and Bu_4NCl , $Bu_4N(CH_3CO_2)$ and 2-methylimidazole to the square-planar iron(II) porphyrin. Employed solvents are listed in Tables. $(F_{20}-TPP)Fe(II)CO$ was prepared from the reaction of 1 atm CO gas with square-planar $(F_{20}-TPP)Fe(II)$ in CD_2Cl_2 .¹⁸

The 5,10,15,20-tetrakis(pentafluorophenyl) porphyrinatoiron(III) chloride, $(F_{20}-TPP)Fe(III)Cl$, (Aldrich Chemical) was crystallized from a 4 mM toluene solution contained in a septum-sealed 5 mm NMR tube. The sample tube was placed in a nitrogen-filled anaerobic glove-box for one week. Partial evaporation of the solution yielded quality crystals.

Measurements

Fluorine-19 and proton NMR spectra of iron porphyrin solutions were recorded at 25 °C on Bruker MSL-300 or Bruker AC-300 spectrometers. A fluorine frequency of 282.3 MHz was used. Chemical shifts are referenced to CFCl_3 (F-19 NMR) and $(\text{CH}_3)_4\text{Si}$ (proton NMR) and downfield shifts are given a positive sign. Concentrations of iron porphyrins ranged from 1.0 mM to 10.0 mM.

Structure determination

Needle-like purple crystal, $0.48 \times 0.28 \times 0.20 \text{ mm}^3$, was mounted in a thin-walled glass capillary on an Enraf-Nonius CAD-4 diffractometer. Preliminary examination and data collection were performed with $\text{MoK}\alpha$ radiation ($\lambda=0.71073 \text{ \AA}$). The structure was determined by the direct methods. Fe

and N atoms were refined with anisotropic thermal motion parameters. All C atoms refine isotropically. All hydrogen atoms were located from electron density difference maps, but were placed at 0.95 \AA from carbon atoms and given isotropic temperature factors 1.1 times that of the atoms to which they were attached. The solvent molecules were modeled by placing C atoms with partial occupancy (0.5 or 0.25) at positions obtained from difference density maps. Those that refined to reasonable isotropic thermal parameters were retained. No attempt was made to sort out proper connectivity. Crystallographic data and details of the data collection are given in Table 1. Final atomic positions for non-hydrogen and hydrogen atoms

Table 1. Phenyl-fluorinated Iron Porphyrin Complexes

spin & oxidn states	species	phenyl fluorine, ppm			pyrrole-H ppm
		ortho	meta	para	
Free ligand	(F ₂₀ -TPPH ₂)	-137.3	-162.1	-152.2	^b
H. S. Fe(III)	(F ₂₀ -TPP)FeCl	-102.0	-152.1	-147.2	81.9 ^b
		-105.1	-154.6		
H. S. Fe(III)	(F ₂₀ -TPP)FeOH	-104.0	-155.0	-148.5	81.0 ^c
			-157.0		
Fe(III) dimer	[(F ₂₀ -TPP)Fe] ₂ O	133.9	162.1	-152.9	14.0 ^b
		-136.2	-164.2		
L. S. Fe(III)	(F ₂₀ -TPP)FePh	-143.8	164.4	-154.0	-18.5 ^c
		-146.2			
L. S. Fe(III)	(F ₂₀ -TPP)FcBu	-145.4	164.7	-154.7	-20.2 ^c
		-146.5			
L. S. Fe(III)	(F ₂₀ -TPP)FcPr	-143.9	-164.6	-154.5	-21.2 ^c
		-145.2			
L. S. Fe(III)	(F ₂₀ -TPP)FcMe	-143.8	-164.6	-154.4	-20.5 ^c
		-146.3			
H. S. Fe(II)	(F ₂₀ -TPP)Fc(THF) ₂	-140.4	165.3	-157.7	59.0 ^d
H. S. Fe(II)	(F ₂₀ -TPP)FeF ⁻	128.2	-160.9	-154.1	30.1 ^c
		-130.2	-162.5		
H. S. Fe(II)	(F ₂₀ -TPP)FeOH	-130.2	-156.7	-152.4	33.6 ^c
H. S. Fe(II)	(F ₂₀ -TPP)FeCl ⁻	-131.0	-165.1	-157.9	40.7 ^c
		-132.2	-166.0		
H. S. Fe(II)	(F ₂₀ -TPP)Fc(2-Melm)	-127.9	-157.9	149.9	54.3 ^c
S=1 Fe(II)	(F ₂₀ -TPP)Fe	-135.5	-161.4	-152.2	5.8 ^c
L. S. Fe(II)	(F ₂₀ -TPP)Fe(pip) ₂	-137.9	-163.3	-153.7	8.4 ^b
L. S. Fe(II)	(F ₂₀ -TPP)FeCO	-137.7	-162.3	-152.5	8.9 ^b
L. S. Fe(II)	(F ₂₀ -TPP)Fe(CN) ₂ ²⁻	-137.6	-163.6	-53.2	8.9 ^b

^aSpectra taken at 25 °C, referenced to CFCl_3 , ^bIn CD_2Cl_2 solution, ^cIn tol-d_8 solution, ^dIn THF-d_8 solution.

Abbreviation: H. S., high-spin; L. S., low-spin; Ph, C_6H_5 ; Bu, C_4H_9 ; Pr, C_3H_7 ; Et, C_2H_5 ; Me, CH_3 ; pip, piperidine; 2-Melm, 2-methylimidazole.

Table 2. Crystal data and structure refinement for (F₂₀-TPP)Fe(III)Cl

Chemical Formula	C ₄₄ H ₈ Cl F ₂₀ Fe N ₄ · C ₇ H ₆
Formula weight	1155.71
Temperature	295 K
Radiation type	MoK α
Radiation wavelength	0.71073
Crystal system	Monoclinic
Space group	P2 ₁ /n
Unit cell dimensions	a=14.649(3) Å b=12.893(3) Å c=26.185(5) Å β ^d =93.14(2) ^o
Cell volume	4944(3) Å ³
Z	4
Density	1.67 Mg/m ³
Absorption coefficient	4.77 mm ⁻¹
Crystal size	0.48 × 0.28 × 0.20 mm ³
R(F)	0.070
wR(F)	0.092
Goodness-of-Fit on F ²	1.05
θ range for data collection	18 ^o to 28 ^o
Reflections collected	13278
Independent reflections	8619
Scan range	0.35 tan θ
Scan speed	5.0 in ω (deg/min)
Index range	-17 ≤ k ≤ 17, -15 ≤ l ≤ 9 -31 ≤ i ≤ 0

^a α and γ were constrained to be 90^o in the refinement of cell parameters.

are listed in Table 2. Table 3 shows bond lengths and angles.

RESULTS AND DISCUSSION

Fluorine-19 NMR spectra for a number of known iron(III) and iron(II) are examined here. The spectrum for (F₂₀-TPP)Fe(III)Cl is shown in Fig. 1. Signals were assigned by examination of the 2,6-F and 3,5-F phenyl-substituted analogues and by consideration of linewidths. Broad *o*-phenyl fluorine signals are located at -102.0 ppm and -105.1 ppm. The meta-phenyl fluorine signals are also split into two components with a separation of 2.5 ppm. The *ortho*- and meta-phenyl fluorine signal splitting is well beyond usual fluorine-fluorine coupling constants, and is best explained by inequivalence of phenyl fluorine groups

Table 3. Atomic coordinates and equivalent isotropic displacement parameters (Å²) for 5, 10, 15, 20-tetrakis (pentafluorophenyl) porphinatoiron(III) chloride

atom	x	y	z	U(eq) or U*
Fe	0.4625(1)	0.4221(1)	0.29395(6)	0.0476(4)
Cl	0.3381(2)	0.4745(3)	0.3292(1)	0.0733(10)
F(22)	0.3441(6)	0.1042(6)	0.4119(3)	0.1038(3)
F(23)	0.3524(8)	-0.0667(8)	0.4678(4)	0.1431(4)
F(24)	0.5112(9)	-0.1763(6)	0.4767(3)	0.1494(4)
F(25)	0.6554(8)	-0.1173(7)	0.4232(4)	0.1368(4)
F(26)	0.6441(6)	0.0534(7)	0.3658(4)	0.1127(4)
F(32)	0.8147(5)	0.5671(7)	0.3786(3)	0.0975(3)
F(33)	0.9132(6)	0.6574(8)	0.4556(4)	0.1178(4)
F(34)	0.8323(6)	0.7129(7)	0.5429(3)	0.1267(3)
F(35)	0.6502(7)	0.6775(7)	0.5507(3)	0.1115(4)
F(36)	0.5538(5)	0.5894(6)	0.4730(3)	0.0785(3)
F(42)	0.3692(7)	0.7937(8)	0.2075(4)	0.1380(4)
F(43)	0.3743(8)	0.9511(7)	0.1414(4)	0.1494(4)
F(44)	0.5115(7)	0.9662(7)	0.0768(3)	0.1229(4)
F(45)	0.6456(7)	0.8216(9)	0.0811(4)	0.1710(4)
F(46)	0.6395(7)	0.6626(8)	0.1462(4)	0.1431(4)
F(52)	0.1575(6)	0.3126(7)	0.1849(3)	0.0937(3)
F(53)	0.0518(5)	0.2132(7)	0.1144(3)	0.0937(3)
F(54)	0.1280(6)	0.0944(7)	0.0437(3)	0.1013(3)
F(55)	0.3108(6)	0.0798(7)	0.0413(3)	0.1051(3)
H(2)	0.6059	0.2078	0.4431	0.0633
H(3)	0.6762	0.3803	0.4553	0.0633
H(7)	0.6671	0.7327	0.3506	0.0633
H(8)	0.6084	0.7799	0.2642	0.0506
H(12)	0.3993	0.6008	0.1193	0.0760
H(13)	0.3252	0.4280	0.1082	0.0760
H(17)	0.3066	0.0911	0.2216	0.0760
H(18)	0.3802	0.0333	0.3038	0.0633

U* is for hydrogen atoms.

with respect to axial ligation at the iron center. Phenyl groups are orthogonal to the porphyrin plane and phenyl group rotation is slow on the 282 MHz NMR time scale. Observation of *ortho*- and/or meta-phenyl fluorine signal splitting provides useful information with regard to the symmetry of axial ligation. However, absence of phenylfluorine signal splitting can not be taken as an indicative of symmetric axial ligation, as the splitting may not be resolved due to large linewidths. Hence, among the five-coordinate high-spin iron(III) derivatives the fluoride and hydroxide complexes show larger linewidths (due to lower zero-field-splitting) than

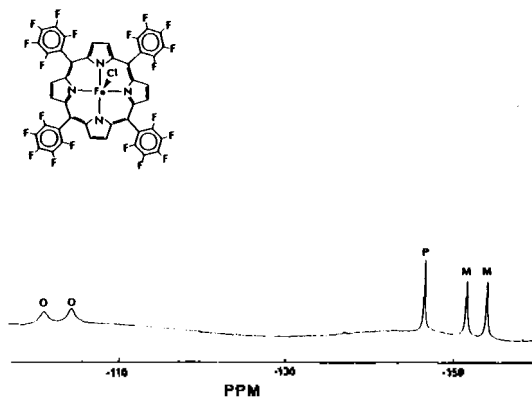


Fig. 1. F-19 NMR spectrum of $(F_{20}\text{-TPP})\text{Fe(III)Cl}$.

does the chloride complex. Phenyl signal splitting is resolved for the chloride complexes, but none is evident (at 282 MHz) for the fluoride complex.

Sizable and often distinctive paramagnetic chemical shifts are evident for phenyl fluorine resonances of high-spin iron(III) porphyrins. For example, downfield shifts of 34.9 and 5 ppm are seen for m, p signals, respectively for $(F_{20}\text{-TPP})\text{Fe(III)Cl}$ as compared with the metal-free porphyrin or diamagnetic $(F_{20}\text{-TPP})\text{Fe(II)CO}$ complex. The greatly attenuated F-19 paramagnetic shifts seen for the dimeric iron(III) complexes in Table 1 are well understood in terms of the antiferromagnetic coupling through the oxo-bridge.

A group of organometallic complexes of $(F_{20}\text{-TPP})\text{Fe(III)}$ were prepared as representative of the low-spin iron(III) state (Table 1). These species are five-coordinate and lack of axial symmetry is associated with splitting of the ortho-phenyl signal (no splitting of the meta-phenyl signal was resolved). Maximum paramagnetic chemical shifts of approximately 9 ppm are seen for the low-spin complexes, and it should be emphasized that shifts are in the upfield direction. Chemical shift differences are quite small among the aryl- and alkyl- $(F_{20}\text{-TPP})\text{Fe(III)}$ complexes listed in Table 2. Low-spin bis-imidazole complexes of iron(III) porphyrins have been described extensively,³ but efforts to generate such complexes of $(F_{20}\text{-TPP})\text{Fe(III)}$ resulted in autoreduction to the iron(II) porphyrin.

The F-19 NMR spectrum of the $S=2(F_{20}\text{-TPP})\text{Fe}$

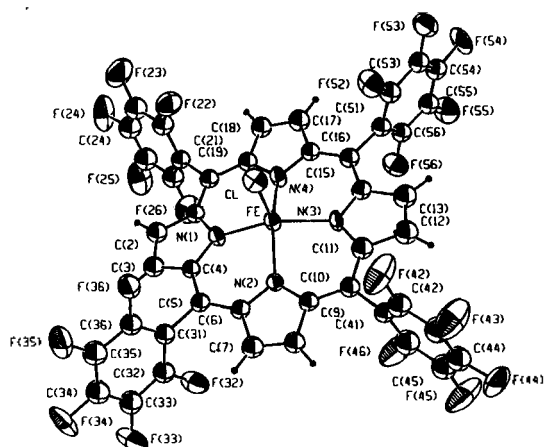


Fig. 2. An ORTEP drawing of the crystal structure of 5, 10, 15, 20-tetrakis(pentafluorophenyl) porphinatoiron(III) chloride.

$(\text{II})\text{F}^-$ complex in CD_2Cl_2 solution at 25°C shows split ortho-phenyl fluorine signals at -128.2 ppm and -132.0 ppm. Meta- and para-phenyl fluorine signals are located at -160.9 ppm, -162.5 ppm (meta), and -154.1 ppm (para).

The other two five-coordinate anionic high spin iron(II) complexes exhibit comparable ortho-fluoro chemical shift values, but considerable differences in meta-fluoro signal positions. In this instance the meta-signal for the OH^- complex is downfield and that for the Cl^- complex is upfield of the signal for the diamagnetic reference compound. In spite of the correlation between pyrrole proton chemical shift values and the basicity of the axial ligand for five-coordinate anionic complexes, the phenyl fluorine resonances appear to exhibit no systematic trend. Additional variability in ortho-fluoro chemical shift values for high-spin iron(II) complexes is evident for the neutral five-coordinate 2-methylimidazole complex with the signal shifted 10 ppm downfield, and for the six-coordinate bis-THF complex with the ortho-fluoro signal 3 ppm upfield of that for a diamagnetic analogue.

Iron(II) porphyrins also may exist in an unusual "intermediate" spin=1 state in the absence of ligands in non-coordinating solvents. Phenyl proton NMR signals for such square-planar species ex-

hibit large shifts due to magnetic anisotropy and associated dipolar shift contributions. Corresponding phenyl F-19 signals show surprisingly small downfield shifts, even though the pyrrole proton signal for $(F_{20}\text{-TPP})\text{Fe(II)}$ is consistent with the $S=1$ formulation.³

Low-spin diamagnetic iron(II) complexes of $(F_{20}\text{-TPP})\text{Fe(II)}$ were generated by addition of two piperidine ligands, by CO coordination, and by cyanide coordination. Chemical shift values for these complexes and free-base ligands differ by no more than 1.0 ppm. The F-19 spectrum of $(F_{20}\text{-TPP})\text{Fe(II)}(\text{CN})_2$ exhibits only residual multiplet structure due to F-19 spin-spin coupling. A concentration of the reasonably high molecular weight of the complex, the viscous DMSO solvent, and F-19 chemical shift anisotropy at 282 MHz presumably gives linewidths that are too large for resolution of spin-spin coupling.

The title compound represents a "benchmark" example of the electron-deficient metalloporphyrins due to its synthetic accessibility, symmetry, and fluorine NMR spectroscopic possibilities. Related work has been performed for the M-oxo dimer, $(F_{20}\text{-TPP})\text{Fe(III)}\text{-O-Fe(III)}(F_{20}\text{-TPP})$.¹⁹ This compound did exhibit somewhat elongated pyrrole nitrogen-Fe distances and a large displacement of the iron atom from the porphyrin plane, but the Fe-O bond distance was equivalent to that of the unsubstituted μ -oxoiron(III) tetraphenylporphyrin dimer. The additional steric interactions offered by fluoro-phenyl groups in the dimeric compound complicate the interpretation of structural changes attributable to the porphyrin electronic perturbations. Hence, a case is made for structural characterization of monomeric $(F_{20}\text{-TPP})\text{Fe(III)Cl}$.

The porphyrin core structural parameters for $(F_{20}\text{-TPP})\text{Fe(III)Cl}$ are surprisingly similar to those of $(\text{TPP})\text{Fe(III)Cl}$. Iron-chlorine and iron-nitrogen distances of 2.19 Å and 2.05 Å, respectively, are equivalent to those in the unsubstituted compound.²⁰ Pyrrole nitrogen-alpha-carbon and alpha carbon-meso carbon distances are respectively the same in the two compounds. Differences are noted for the out-of-plane displacement of the iron atom, with

Table 4. Bond lengths (Å) and angles (deg) for 5, 10, 15, 20-tetrakis(pentafluorophenyl) porphinatoiron(II) chloride

Fe-Cl	2.194(4)	Fe-N(1)	2.052(9)
Fe-N(2)	2.059(9)	Fe-N(3)	2.050(9)
Fe-N(4)	2.068(9)	F(22)-C(22)	1.33(2)
F(23)-C(23)	1.35(2)	F(24)-C(24)	1.38(2)
F(25)-C(25)	1.37(2)	F(26)-C(26)	1.31(2)
F(32)-C(32)	1.35(2)	F(33)-C(33)	1.34(2)
F(34)-C(34)	1.37(2)	F(35)-C(35)	1.32(2)
F(36)-C(36)	1.32(1)	F(42)-C(43)	1.32(2)
F(43)-C(43)	1.35(2)	F(44)-C(44)	1.35(2)
F(45)-C(45)	1.32(2)	F(46)-C(46)	1.33(2)
F(52)-C(52)	1.36(2)	F(53)-C(53)	1.35(2)
F(54)-C(54)	1.34(1)	F(55)-C(55)	1.35(2)
F(56)-C(56)	1.33(1)	N(1)-C(1)	1.36(1)
N(1)-C(4)	1.37(1)	N(2)-C(6)	1.38(1)
N(2)-C(9)	1.37(1)	N(3)-C(11)	1.37(2)
N(3)-C(14)	1.36(1)	N(4)-C(16)	1.36(1)
N(4)-C(19)	1.38(1)	Cl-Fe-N(1)	103.5(3)
Cl-Fe-N(2)	104.1(3)	Cl-Fe-N(3)	102.2(3)
Cl-Fe-N(4)	100.5(3)	N(1)-Fe-N(2)	87.7(4)
N(1)-Fe-N(3)	154.3(4)	N(1)-Fe-N(4)	87.3(4)
N(2)-Fe-N(3)	86.9(3)	N(2)-Fe-N(4)	155.4(4)
N(3)-Fe-N(4)	87.3(4)	Fe-N(1)-C(1)	127.5(8)
Fe-N(1)-C(4)	126.0(8)	C(1)-N(1)-C(4)	105.6(9)
Fe-N(2)-C(6)	126.0(8)	Fe-N(2)-C(9)	127.2(7)
C(6)-N(2)-C(9)	105.6(9)	Fe-N(3)-C(11)	126.7(8)
Fe-N(3)-C(14)	125.8(8)	C(11)-N(3)-C(14)	106.0(1)
Fe-N(4)-C(16)	126.1(8)	Fe-N(4)-C(19)	126.6(8)
C(16)-N(4)-C(19)	105.0(1)	N(1)-C(1)-C(2)	110.0(1)
N(1)-C(1)-C(20)	126.0(1)	N(1)-C(4)-C(3)	110.0(1)
N(1)-C(4)-C(5)	126.0(1)	N(2)-C(6)-C(5)	126.0(1)
N(2)-C(6)-C(7)	110.0(1)	N(2)-C(9)-C(8)	110.0(1)
N(2)-C(9)-C(10)	126.0(1)	N(3)-C(11)-C(10)	126.0(1)
N(3)-C(11)-C(12)	110.0(1)	N(3)-C(14)-C(13)	111.0(1)

the value of 0.45 Å for $(F_{20}\text{-TPP})\text{Fe(III)Cl}$ and 0.39 Å for $(\text{TPP})\text{Fe(III)Cl}$ with respect to the pyrrole nitrogen plane. The larger iron displacement for the fluorinated compound matches that seen for the oxo-bridged dimer noted above. The significance of this additional iron displacement is uncertain, as values cover a wider range for halide complexes of iron(III) porphyrins.²¹ One additional significant bond distance difference is seen for the fluorinated derivative in that the pyrrole β -carbon-carbon distance is 1.34 Å for $(F_{20}\text{-TPP})\text{Fe(III)Cl}$ and 1.38 Å for $(\text{TPP})\text{Fe(III)Cl}$. Overall the minor structural

changes seen for the electron-deficient iron porphyrin compound do not parallel the dramatic reactivity perturbations.

In conclusion, large chemical shifts for the ortho-fluorine signals of iron tetrakis(pentafluorophenyl) porphyrin complexes were observed. The fluorine-19 NMR chemical shift values depend on the electronic and spin states in the ferric and ferrous porphyrins. Analysis of isotropic shifts of the iron(III) porphyrin using fluorine-19 NMR indicates there is a sizable contact contribution at the ortho-fluorine phenyl ring position. Large chemical shift values of the phenyl fluorine, which are sensitive to the oxidation and spin state, can be utilized for identification of the solution electronic structures of iron(III) and iron(II) porphyrins. Large-splittings of ortho- and meta-fluorine signals compared to those of the phenyl proton signals provide useful information about the stoichiometry of ligand binding in that split signals are indicative of asymmetry along the vertical axis of the iron porphyrin complex. The title compound was also structurally characterized in an attempt to relate molecular structure properties with oxidative catalytic and high affinity ligand binding properties.

Acknowledgment. Financial supports in part from SunMoon University(96) and in part from MRRC(96A-16-05-03-2) are gratefully acknowledged. Thanks are given to Prof. H. M. Goff for the helpful discussion.

Supplementary Material Available. Tables of observed and calculated factors (98 pages) are available from B.-H. S

REFERENCES

1. a) Traylor, P. S.; Dolphin, D.; Traylor, T. G. *J. Chem. Soc., Chem. Commun.* **1984**, 279-280. b) Chang, C. K.; Ebina, F. *J. Chem. Soc., Chem. Commun.* **1985**, 779-780.
2. Nanthakumar, A.; Goff, H. M. *J. Am. Chem. Soc.* **1990**, *112*, 4047-4049.
3. Song, B. H.; Goff, H. M. (unpublished data)
4. La Mar, G. N.; Walker, F. A. *The Porphyrins*, D. Dolphin, Ed.; p 61, Academic Press: New York, IV, 1979.
5. Goff, H. M. *Iron Porphyrins - Part I*; Lever, A. B. P.; Gray, H. B. Eds.; Addison - Wesley: Reading, MA, 1982; p 237.
6. Walker, F. A.; Ursula Simonis, *Biological Magnetic Resonance*; Berliner, L. J.; Reuben, J. Eds.; Plenum Press: **1993**, *12*, 133.
7. Mispelter, J.; Momenteau, M.; Lhoste, J. -M. *Biological Magnetic Resonance*; Berliner, L. J.; Reuben, J. Eds.; Plenum Press: **1993**, *12*, 299.
8. Nanthakumar, A.; Goff, H. M. *J. Am. Chem. Soc.* **1990**, *112*, 4047.
9. Chang, C. K.; Ebina, F. *J. Chem. Soc., Chem. Commun.* **1985**, 779.
10. Traylor, P. S.; Dolphin, D.; Traylor, T. G. *J. Chem. Soc., Chem. Commun.* **1984**, 279.
11. Ellis, P. E.; Lyons, J. E. *Coord. Chem. Rev.* **1990**, *105*, 181.
12. Perrin, D. D.; Armarego, W. L. F.; Perrin, D. R. *Purification of Laboratory Chemicals*, 2nd Ed.; Pergamon Press: New York, 1980.
13. Furniss, B. S.; Hannaford, A. J.; Rogers, V.; Smith, P. W. G.; A. R. Tatchell, *Vogel's Textbook of Practical Organic Chemistry*, 4th Ed.; The Chauer Press, Ltd.: Suffolk, 1978; p 78.
14. Guillard, R.; Lecomte, C.; Kadish, K. M. *Structure and Bonding*, **1987**, *64*, 205.
15. Cheng, R. T.; Latos-Grazynski, L.; Balch, A. L. *Inorg. Chem.* **1982**, *21*, 2412.
16. Shin, K.; Kramer, K.; Goff, H. M. *Inorg. Chem.* **1987**, *26*, 4103.
17. Yu, B. -S.; Goff, H. M. *J. Am. Chem. Soc.* **1989**, *111*, 6558.
18. a) Landrum, J. T.; Hatano, K.; Scheidt, W. R.; Reed, C. A. *J. Am. Chem. Soc.* **1980**, *102*, 6729. b) Arafa, I. M.; Shin, K.; Goff, H. M., *J. Am. Chem. Soc.* **1988**, *110*, 5228.
19. Gold, A.; Jayaraj, K.; Doppelt, P.; Fischer, J.; Weiss, R. *Inorg. Chim. Acta.* **1988**, *150*, 177-181.
20. Hoard, J. L.; Cohen, G. H.; Click, M. D., *J. Am. Chem. Soc.* **1967**, *89*, 1992-1996.
21. Hatano, K.; Scheidt, W. R. *Inorg. Chem.* **1979**, *18*, 877-879.